## References

1. Vargha-Khadem F, O'Gorman AM, Watters GV. Aphasia and handedness in relation to hemispheric side, age at injury and severity of cerebral lesion during childhood. Brain 1985;108: 677–696.
2. Vargha-Khadem F, Isaacs E, Muter V. A review of cognitive outcome after unilateral lesions sustained during childhood. J Child Neurol 1994;9(suppl 2):67–73.
3. Hertz-Pannier L, Chiron C, Jambaque I, et al. Late plasticity for language in a child's non-dominant hemisphere: a pre- and post-surgery fMRI study. Brain 2002;125:361–372.
4. Muller RA, Rothermel RD, Behen ME, et al. Language organization in patients with early and late left-hemisphere lesion: a PET study. Neuropsychologia 1999;37:545–557.
5. Liegeois F, Connelly A, Cross JH, et al. Language reorganization in children with early-onset lesions of the left hemisphere: an fMRI study. Brain 2004;127:1229–1236.
6. McCandliss BD, Cohen L, Dehaene S. The Visual Word Form Area: expertise for reading in the fusiform gyrus. Trends Cogn Sci 2003;7:293–299.
7. Aghababian V, Nazir TA. Developing normal reading skills: aspects of the visual processes underlying word recognition. J Exp Child Psychol 2000;76:123–150.
8. Shaywitz BA, Shaywitz SE, Pugh KR, et al. Disruption of posterior brain systems for reading in children with developmental dyslexia. Biol Psychiatry 2002;52:101–110.
9. Gaillard WD, Balsamo LM, Ibrahim Z, et al. fMRI identifies regional specialization of neural networks for reading in young children. Neurology 2003;60:94–100.
10. Cohen L, Martinaud O, Lemer C, et al. Visual Word Recognition in the left and right hemispheres: anatomical and functional correlates of peripheral alexias. Cereb Cortex 2003;13: 1313–1333.
11. Cohen L, Henry C, Dehaene S, et al. The pathophysiology of letter-by-letter reading. Neuropsychologia 2004;42:1768–1780.
12. Dehaene-Lambertz G, Dehaene S, Hertz-Pannier L. Functional neuroimaging of speech perception in infants. Science 2002; 298:2013–2015.
13. Balsamo LM, Xu B, Grandin CB, et al. A functional magnetic resonance imaging study of left hemisphere language dominance in children. Arch Neurol 2002;59:1168–1174.
14. Gaillard WD, Hertz-Pannier L, Mott SH, et al. Functional anatomy of cognitive development: fMRI of verbal fluency in children and adults. Neurology 2000;54:180–185.
15. Patterson K, Vargha-Khadem F, Polkey CE. Reading with one hemisphere. Brain 1989;112:39–63.
16. Comi AM. Pathophysiology of Sturge-Weber syndrome. J Child Neurol 2003;18:509–516.
17. Di Virgilio G, Clarke S. Direct interhemispheric visual input to human speech areas. Hum Brain Mapp 1997;5:347–354.


# In Vivo Detection of Microglial Activation in Frontotemporal Dementia


Annachiara Cagnin, MD,[1,2] Martin Rossor, MD, FRCP,[3] Elizabeth L. Sampson, MD,[3] Toby MacKinnon, MBBS,[1] and Richard B. Banati, MD[1,4,5]



**Using positron emission tomography and [$^{11}$C](*R*)-PK11195, a marker of "peripheral benzodiazepine sites" that is upregulated on activated microglia during progressive tissue pathology, we show increased binding of [$^{11}$C](*R*)-PK11195 in frontotemporal lobar degeneration in the typically affected frontotemporal brain regions. This implies the presence of an active glial response reflecting progressive neuronal degeneration. It also suggests that increased [$^{11}$C](*R*)-PK11195 binding, previously demonstrated for Alzheimer's disease, may occur independently from increased amyloid plaque formation, given that it is not a characteristic feature of frontotemporal lobar degeneration.**



Ann Neurol 2004;56:894–897


Frontotemporal lobar degeneration (FTLD) is characterized by focal atrophy of the temporal and frontal lobes.[1] Three main histopathological features are found: nonspecific changes of neuronal loss, microvacuolation, and gliosis; τ deposition including Pick bodies; and ubiquitin-positive, τ-negative inclusions.[2,3] Glial changes including activated microglia are common, but, unlike Alzheimer's disease (AD), increased amyloid plaque formation is usually not seen.[4,5]

The isoquinoline PK11195 is a ligand for the "peripheral benzodiazepine binding site" that is particularly abundant in cells of mononuclear-phagocyte lineage. High-resolution, single-cell, [$^{3}$H](*R*)-PK11195 autoradiography combined with immunocytochemical


From the [1]MRC Cyclotron Unit, MRC Clinical Sciences Centre, Imperial College London, Hammersmith Hospital Campus, London, United Kingdom; [2]Department of Neurosciences, University of Padova, Padova, Italy; [3]Dementia Research Group, Institute of Neurology Queen Square, London, United Kingdom; [4]Department of Neuropathology, Imperial College School of Medicine, Charing Cross Hospital, London, United Kingdom; and [5]School of Medical Radiation Sciences and Ramaciotti Center for Brain Imaging (Brain Mind Research Institute), University of Sydney, Sydney, New South Wales, Australia.



Received Apr 26, and in revised form Aug 4 and Sep 30. Accepted for publication Sep 30, 2004.

Published online Nov 24, 2004, in Wiley InterScience (www.interscience.wiley.com). DOI: 10.1002/ana.20332



Address correspondence to Dr Banati, Chair of Medical Radiation Sciences, University of Sydney, East Street, PO Box 170, Lidcombe, New South Wales 1825, Australia. E-mail: r.banati@fhs.usyd.edu.au

double-labeling in experimental models and on human tissue has shown that brain binding of the (*R*)-enantiomer of PK11195 closely follows the distribution of activated microglia rather than astrocytes.[6] In vivo, in the absence of blood–brain barrier disruption, this is also likely to hold true, indicating that [$^{11}$C](*R*)-PK11195 positron emission tomography (PET) should provide a useful marker of activated microglia. We have previously shown focally increased [$^{11}$C](*R*)-PK11195 signals in multiple sclerosis and Rasmussen's encephalitis, but such increases were not observed in inactive tissue pathology, such as burnt-out multiple sclerosis plaques, or in scar tissue, such as that found in stable epilepsy patients with hippocampal sclerosis characterized by reactive astrogliosis.[6] After cerebral ischemia, increased [$^{3}$H]PK11195 binding is observed in and around the infarcted tissue where it colocalizes with brain macrophages of either microglial or blood-borne origin.[7] Importantly, it is also regularly found in areas remote from the primary ischemic lesion and with intact brain barrier, particularly in the thalamus. This demonstrates that microglial activation also occurs in areas that are linked to the primary lesion site by retrograde and anterograde projectioning neuronal fiber tracts, an observation that has been suggested as one cell-biological correlate of diaschisis.[8]

In our previous study of patients with mild AD, [$^{11}$C](*R*)-PK11195 binding was increased in entorhinal, temporoparietal, and posterior cingulate cortex, supporting the notion that AD pathology is associated with an early inflammatory response in the form of microglial activation.[9] However, it remained unclear whether the increased [$^{11}$C](*R*)-PK11195 signal reflected the glial response to amyloid aggregation or could also occur in other dementias without increased plaque formation, and hence be more directly linked to the process of neuronal degeneration.[9]

## Subjects and Methods

### *Subjects*

Patients were recruited from the Specialist Cognitive Disorders Clinic, National Hospital for Neurology and Neurosurgery (London, UK). We studied five patients with FTLD diagnosed using established consensus criteria.[1] In clinicopathological series, these diagnostic criteria were shown to have good sensitivity (FTLD diagnosed or strongly considered at first presentation in 80% of autopsy-proven cases) and a specificity of 97% in distinguishing correctly patients with FTLD from AD patients.[10] Beyond this, the diagnostic accuracy of all patients was further assured by a minimally once annual clinical follow-up over a period of 3 to 6 years, consisting of repeated neurological and neuropsychological assessments and longitudinal volumetric brain scans, as well as further follow-up confirmation after this study. In addition to the exclusion criteria specified by Neary and colleagues,[1] we excluded patients at an advanced stage of FTLD and those with magnetic resonance imaging (MRI) evidence of vascular lesions or other focal brain lesions.

Clinically, four patients had symptoms of progressive nonfluent aphasia, and MRI showed predominant temporal lobe atrophy; one patient had a dysexecutive and behavioral syndrome, relative preservation of language functions, and atrophy of the frontal pole. Mean age at onset was 56 years. Median disease duration was 4 years with an interquartile range of 2 years. At the time of the PET studies, the mean age was 61 years (range, 58–69; interquartile range, 4). The mean Mini-Mental State Examination score was 26 (range, 23–30), indicating that the patients had a mild degree of cognitive impairment, with one patient, the aforementioned patient with relative preservation of language functions, scoring 30 of 30 in this assessment. Eight age-matched healthy volunteers were scanned as a control group (median age, 62 years; interquartile range, 18).

### *Methods*

Each patient underwent an [$^{11}$C](*R*)-PK11195 PET scan (ECAT 953B scanner; CTI/Siemens, Knoxville, TN) and a volumetric T1-weighted MR brain scan (1.0 Tesla, Picker, Cleveland, OH) on the same day. Dynamic PET data were acquired and analyzed as previously described.[6,9] Because pathological changes in FTLD may be widespread throughout the brain, the anatomical a priori identification of an unaffected reference region might be inappropriate. Therefore, as in a previous study of patients with AD,[9] the parametric images of [$^{11}$C](*R*)-PK11195 binding potential were generated using a basis-function implementation of a simplified reference-tissue model, whereby the reference input function is extracted only from those voxels in whom the kinetic behavior of the ligand had normal characteristics seen in healthy cortex.[6,9] In this study, the extracted normal input functions showed no systematic differences to those previously used in AD (ie, there were no significant differences in the shapes of the input kinetics from the individual FTLD patients and the mean population input kinetic from the AD patients, underlying the previously published regional mean binding potential values with $\chi^2$ test always yielding $p < 0.0001$).[9] The parametric images of [$^{11}$C](*R*)-PK11195 binding potential were used for a volume of interest analysis of regional mean binding. Before application to the PET parametric images, volumes of interest corresponding to anatomical subdivision of the temporal lobe, dorsolateral prefrontal cortex, parietal lobule, posterior and anterior cingulate, insula, and subcortical regions were drawn on the individual volumetric MRI by an observer blinded to subjects' details and the results of the individual PET scans who was following published criteria.[9] Mean, standard deviation, and *Z*-scores were calculated to determine the significance of the regional increase in [$^{11}$C](*R*)-PK11195 binding in each patient compared with the control subjects. *Z*-scores greater than 1.6 (in the one-tailed *Z*-test, testing for increase in specific binding) were considered significant ($p < 0.05$).

Three dimensional, T1-weighted, brain MRI scans were obtained for coregistration with PET images and exclusion of incidental pathology.

## Results

All FTLD patients showed asymmetric, predominantly left temporal atrophy extending into the ipsilateral fron-

tal lobe and varying patterns of either unilateral or bilateral increased [$^{11}$C](*R*)-PK11195 binding in cortical frontal, mesial temporal, and subcortical regions, as shown in the Figure.

On group analysis, mean [$^{11}$C](*R*)-PK11195 binding potentials were significantly increased in the left dorsolateral prefrontal cortex, the right hippocampus and parahippocampus, and in the putamen bilaterally (Table). A trend toward significance was found in the left hemisphere in the following regions: the fusiform ($p$ = 0.08) and inferior temporal gyri ($p$ = 0.08), inferior parietal ($p$ = 0.07), and posterior cingulate cortex ($p$ = 0.08). Similar to previous findings,[6,9] [$^{11}$C](*R*)-PK11195 binding was observed in pons and midbrain, which in the group analysis, however, did not reach the level of statistical significance.

## Discussion

This pronounced frontotemporal pattern of microglial activation detected by [$^{11}$C](*R*)-PK11195 PET in our cohort of FTLD patients differed from that previously reported for AD patients in whom the increased [$^{11}$C](*R*)-PK11195 binding was found primarily in temporal, parietal, and posterior cingulate regions.[9] With respect to the temporal lobe, the previously reported AD patients showed increased [$^{11}$C](*R*)-PK11195 binding most consistently in the inferior temporal gyrus, whereas the significant increases in this study's group of FTLD patients localized to the entorhinal cortex. Our finding of bilaterally increased putamen [$^{11}$C](*R*)-PK11195 uptake in FTLD agrees with published neuropathological data showing frequent involvement of the basal ganglia.[4] The frontotemporal distribution of regions found in group analysis to have increased [$^{11}$C](*R*)-PK11195 binding matched the predominantly left hemispheric pattern of brain atrophy seen in FTLD patients, but group analysis also showed increased [$^{11}$C](*R*)-PK11195 binding in the right hemisphere. In accordance with previous observations, this suggests that microglial activation is indeed present at stages of tissue pathology before marked macroscopic changes in brain anatomy have occurred. The failure to detect significantly increased [$^{11}$C](*R*)-PK11195 binding in left mesial temporal regions may reflect signal loss because of severe atrophy. Alternatively, it may indicate that a previously active disease process associated with microglial activation had burnt out, resulting in a reduction of activated microglia, as postmortem investigations of FTLD brains have indeed suggested.[4]

Extending previous studies in AD, a condition characterized by a high load of amyloid plaques, our observation in FTLD, which is not usually associated with an increased amyloid deposition, suggests that glial responses are a general phenomenon of neurodegenerative diseases that do not depend specifically on the presence of amyloid plaques. Thus, the neuronal loss and axonal degeneration seen in FTLD is sufficient to induce microglial activation. Although our results have confirmed that the distribution pattern of microglial activation conforms with the pattern of clinical impairment, which in the case of FTLD is associated with speech and behavioral difficulties, they also highlight the variability among patients. This is likely to reflect the considerable neuropathological heterogeneity within the group of FTLD patients. Further studies are needed to clarify the extent to which the pattern of glial tissue pathology beyond certain core areas, such as left frontotemporal regions, relates to inherent disease heterogeneity or is the result of different stages of disease progression.

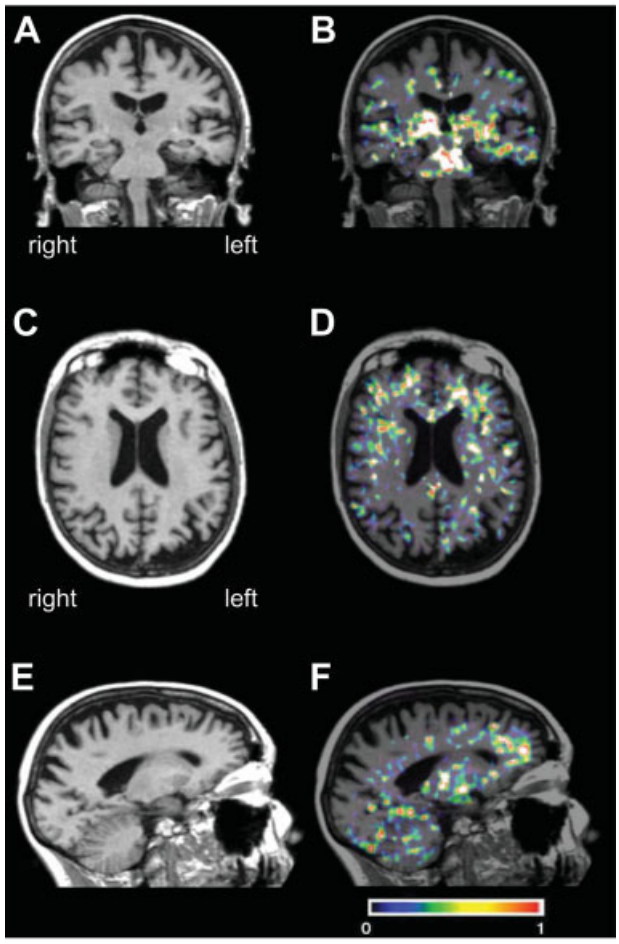


*Fig. First and second column show [$^{11}$C](R)-PK11195 positron emission tomography images (B, D, F) of a patient with frontotemporal lobar degeneration (FTLD; age, 69 years; disease duration, 3 years) coregistered to patient's magnetic resonance imaging scans (A, C, E). In this patient, a significant increase of [$^{11}$C](R)-PK11195 binding is seen in the left frontal and temporal lobes (B, D) overlapping with the area of atrophic changes. Widespread [$^{11}$C](R)-PK11195 binding is seen also in areas with less obvious volume loss, such as the right frontal cortex, the right mesial temporal lobe, and the basal ganglia. The color bar denotes [$^{11}$C](R)-PK11195 binding potential values between 0 and 1.*

*Table. Mean (SD) [$^{11}$C](R)-PK11195 Binding Potential in FTLD Patients and Age-Matched Normal Controls*

| Location | Right Hemisphere | | | Left Hemisphere | | |
|---|---|---|---|---|---|---|
| | Controls | FTLD | *p* | Controls | FTLD | *p* |
| Dorsolateral prefrontal cortex | 0.15 (0.06) | 0.22 (0.11) | 0.14 | 0.14 (0.06) | 0.24 (0.11) | 0.05 |
| Superior temporal gyrus | 0.15 (0.03) | 0.17 (0.10) | 0.31 | 0.13 (0.04) | 0.16 (0.14) | 0.32 |
| Inferior and middle temporal gyrus | 0.13 (0.03) | 0.17 (0.12) | 0.26 | 0.13 (0.04) | 0.23 (0.13) | 0.08 |
| Fusiform gyrus | 0.12 (0.04) | 0.19 (0.15) | 0.17 | 0.14 (0.04) | 0.24 (0.14) | 0.08 |
| Parahippocampus | 0.11 (0.06) | 0.25 (0.11) | 0.02 | 0.09 (0.03) | 0.18 (0.11) | 0.08 |
| Hippocampus | 0.14 (0.06) | 0.27 (0.13) | 0.04 | 0.14 (0.05) | 0.21 (0.13) | 0.16 |
| Amygdala | 0.16 (0.06) | 0.22 (0.09) | 0.11 | 0.16 (0.07) | 0.26 (0.20) | 0.17 |
| Insula | 0.16 (0.08) | 0.20 (0.16) | 0.31 | 0.16 (0.05) | 0.13 (0.16) | 0.34 |
| Anterior cingulate gyrus | 0.14 (0.04) | 0.17 (0.11) | 0.34 | 0.14 (0.07) | 0.17 (0.09) | 0.26 |
| Posterior cingulate gyrus | 0.20 (0.07) | 0.24 (0.14) | 0.26 | 0.18 (0.05) | 0.27 (0.12) | 0.08 |
| Inferior parietal lobule | 0.12 (0.05) | 0.19 (0.11) | 0.13 | 0.08 (0.04) | 0.18 (0.12) | 0.07 |
| Pallidum | 0.27 (0.08) | 0.43 (0.19) | 0.07 | 0.26 (0.07) | 0.42 (0.23) | 0.10 |
| Putamen | 0.25 (0.04) | 0.35 (0.10) | 0.04 | 0.26 (0.04) | 0.39 (0.15) | 0.05 |
| Thalamus | 0.44 (0.07) | 0.48 (0.14) | 0.25 | 0.40 (0.06) | 0.49 (0.17) | 0.17 |

SD = standard deviation; FTLD = frontotemporal lobar degeneration.

## References


1. Neary D, Snowden JS, Gustafson L, et al. Frontotemporal lobar degeneration: a consensus on clinical diagnostic criteria. Neurology 1998;51:1546–1554.
2. Uchihara T, Ikeda K, Tsuchiya K. Pick body disease and Pick syndrome. Neuropathology 2003;23:318–326.
3. Munoz DG, Dickson DW, Bergeron C, et al. The neuropathology and biochemistry of frontotemporal dementia. Ann Neurol 2003;54(suppl 15):24–28.
4. Mirra SS, Hyman BT. Ageing and dementia. In: Graham DI, Lantos PL, eds. Greenfield's neuropathology. Vol. 2. London: Arnold, 2002:195–271.
5. Paulus W, Bancher C, Jellinger K. Microglial reaction in Pick's disease. Neurosci Lett 1993;161:89–92.
6. Banati RB, Newcombe J, Gunn RN, et al. The peripheral benzodiazepine binding site in the brain in multiple sclerosis: quantitative in vivo imaging of microglia as a measure of disease activity. Brain 2000;123:2321–2337.
7. Myers R, Manjil LG, Cullen BM, et al. Macrophage and astrocyte populations in relation to [3H]PK 11195 binding in rat cerebral cortex following a local ischaemic lesion. J Cereb Blood Flow Metab 1991;11:314–322.
8. Pappata S, Levasseur M, Gunn RN, et al. Thalamic microglial activation in ischemic stroke detected in vivo by PET and [$^{11}$C]PK11195. Neurology 2000;55:1052–1054.
9. Cagnin A, Brooks DJ, Kennedy AM, et al. In-vivo measurement of activated microglia in dementia. Lancet 2001;358:461–467.
10. Rosen HJ, Hartikainen KM, Jagust W, et al. Utility of clinical criteria in differentiating frontotemporal lobar degeneration (FTLD) from AD. Neurology 2002;58:1608–1615.


 
Published by Wiley-Liss, Inc., through Wiley Subscription Services